Predictability of Mediterranean climate variables from oceanic variability. Part I: Sea surface temperature regimes

E. Hertig · J. Jacobeit

Abstract The determination of specific sea surface temperature (SST) patterns from large-scale gridded SST-fields has widely been done. Often principal component analysis (PCA) is used to condense the SST-data to major patterns of variability. In the present study SST-fields for the period 1950–2003 from the area 20°S to 60°N are analysed with respect to SST-regimes being defined as large-scale oceanic patterns with a regular and at least seasonal occurrence. This has been done in context of investigations on seasonal predictability of Mediterranean regional climate with large-scale SST-regimes as intended predictors in statistical model relationships. The SST-regimes are derived by means of a particular technique including multiple applications of s-mode PCA. Altogether 17 stationary regimes can be identified, eight for the Pacific Ocean, five for the Atlantic Ocean, two for the Indian Ocean, and two regimes which show a distinct co-variability within different ocean basins. Some regimes exist, with varying strength and spatial extent, throughout the whole year, whereas other regimes are only characteristic for a particular season. Several regimes show dominant variability modes, like the regimes associated with El Niño, with the Pacific Decadal Oscillation or with the North Atlantic Tripole, whereas other regimes describe little-known patterns of large-scale SST variability. The determined SST-regimes are subsequently used as predictors for monthly precipitation and temperature in the Mediterranean area. This subject is addressed in Part II of this paper.

E. Hertig (✉) · J. Jacobeit
Institute for Geography, University of Augsburg,
Universitätsstr 10, 86135 Augsburg, Germany
e-mail: elke.hertig@geo.uni-augsburg.de

Keywords Sea surface temperature regimes · Statistical analyses · Monthly predictions · Mediterranean area

1 Introduction

Despite the impossibility to exactly predict the short-term weather conditions beyond a couple of days, it is possible to provide seasonal forecasts in terms of mean conditions and associated uncertainties and probabilities (Dix and Hunt 1995). This is due to the fact that on this time scale slowly varying boundary conditions, especially the sea surface temperatures (SSTs), control the general characteristics of climate. There is already fair evidence for useful climate predictability in equatorial and tropical regions where the noise level is small, but there is only little evidence for it in mid-latitudes. According to a study based on GCM simulations by Rowell (1998), SSTs can generally be used for predictions of precipitation in the northern hemisphere mid-latitudes, mainly in the winter and spring months (with lowest predictability in autumn).

The SST field has been shown to have influence on extratropical circulation patterns and climate, as for example through the tropical El Niño/Southern Oscillation (Moron and Plaut 2003; Lloyd-Hughes and Saunders 2002) and through regional response patterns for extratropical SSTs (Rodriguez-Fonseca et al. 2006, Rodwell et al. 1999, Colman and Davey 1999). To account for the possible effects from different oceanic regions it is necessary to incorporate the SST-patterns preferably on a global scale. Thus, Barnston and Smith (1996) and Hwang et al. (2001) have demonstrated that in the scope of seasonal predictions global SST-fields yield better results compared to the use of local SST-fields.

A considerable number of studies already exist regarding the determination of specific SST-patterns. The El Niño Southern Oscillation (ENSO) is known as the most prominent pattern of inter-annual variability in the global climate system, and a great deal of progress has been made in understanding and predicting ENSO (An 2009; Alexander et al. 2002; Mason and Mimmack 2002; Neelin et al. 1998). Besides ENSO, statistical analyses of SST variations have been performed for particular ocean basins, e.g. by Deser and Blackmon (1993, 1995) for the Atlantic Ocean and for the Pacific Ocean. Often SSTs are studied in combination with an investigation of ocean–atmosphere couplings and associated climate variables, e.g. for the North Pacific region by Zhang et al. (1998) and Wallace et al. (1992), for the North Atlantic region by Cassou et al. (2004), Peng et al. (2003), Czaja and Frankignoul (2002), and for the Indian Ocean for instance by Webster et al. (1999).

Most studies concentrate on the dominant modes of SST-variation. Secondary patterns which do not explain a major fraction of SST variance are not considered. Furthermore, the focus is mostly on a particular season, a tracking of specific SST-modes throughout the year has only rarely been done (e.g. by García-Serrano et al. 2008). In addition, the majority of investigations does not include relations on a global scale and considers only a specific ocean basin.

In the present study SST-fields in the whole area from 20°S to 60°N are analysed during all months of the year. The focus of the investigation is on the spatial and temporal structuring of the SST-variations by means of principal component analysis (PCA). The resulting SST-regimes characterize the intra- as well as the inter-annual evolution of those SST-patterns which clearly step out from the random variations. Thus, a synopsis of the SST-patterns in the Pacific Ocean, Atlantic Ocean, and Indian Ocean in all months of the year for the period 1950–2003 is achieved. The SST-regimes are compiled against the background of using them as predictors for monthly precipitation and temperature in the Mediterranean area.

2 Data

For the characterization of oceanic variability, the global SST data set ERSST, Version 2 (Extended Reconstruction Sea Surface Temperatures, Smith and Reynolds 2003) has been analysed. It is available with a 2° horizontal resolution. ERSST is based on the Comprehensive Ocean Atmosphere Data Set of Woodruff et al. (1998). A comparison of the ERSST data with the HadISST-dataset from the Hadley Centre by Rayner et al. (2003) indicates that both data are highly correlated (correlation coefficients greater than 0.7) after the year 1950, major differences are limited to areas with sparse observational data (southern hemisphere oceans south of 20°S). The ERSST data is also in good agreement with the satellite- and observation-based data of the NOAA OI-Analysis (Reynolds et al. 2002). The high northern latitudes north of 60°N and the southern hemisphere latitudes south of 20°S have been excluded from the present study, considering the relatively low quality and density of the observational data. From the 4,965 grid boxes between 20°S and 60°N only 4,943 are taken for further investigation, because 22 grid boxes at the northern boundary of the study area do not show any temporal variance in the 1950–2003 period (due to the fact that in the original dataset the value of −1.8°C is assigned to a grid box in case of SSTs being lower than this value).

The starting year (1950) of the following analyses results from the availability of high-quality SST-data, the ending year (2003) has been the last complete year at the beginning of this investigation.

3 Determination of sea surface temperature regimes

Figure 1 provides a simplified scheme of the methodology for the determination of the SST-regimes. The assignments of principal components to specific SST-regimes within this scheme are completely arbitrary and have been included only for illustration purposes. The entire procedure includes several steps of analyses:

In a first step s-mode PCA is separately applied to monthly mean, 2-monthly mean, and 3-monthly mean SST fields to obtain specific patterns of SST-variation throughout the year. The multiple-month analyses refer to the overlapping 2-month periods (January/February, February/March,…) and 3-month periods (January/February/March, February/March/April,…). The extraction of principal components (PCs) is based on the correlation matrix of the input variables. The determination of the number of PCs to be extracted follows the approach of Philipp et al. (2007) and is based on the criterion that each PC has to be uniquely representative for at least one input variable. Representativeness is assumed when the maximum loading of a variable on a particular PC is at least one standard deviation greater than the other loadings of this variable on the remaining PCs; additionally, this maximum loading has to be statistically significant at the 95% level. The number of extracted PCs varies between 7 (October–December) and 22 (June/July) with overall explained variances (EVs) between 64 and 87%. Subsequently, the PC loading patterns of the different analyses (for 1-, 2-, and 3-month subperiods) are compared with each other to identify patterns which appear for several months thus being relevant not only for one particular month, but for an extended period of

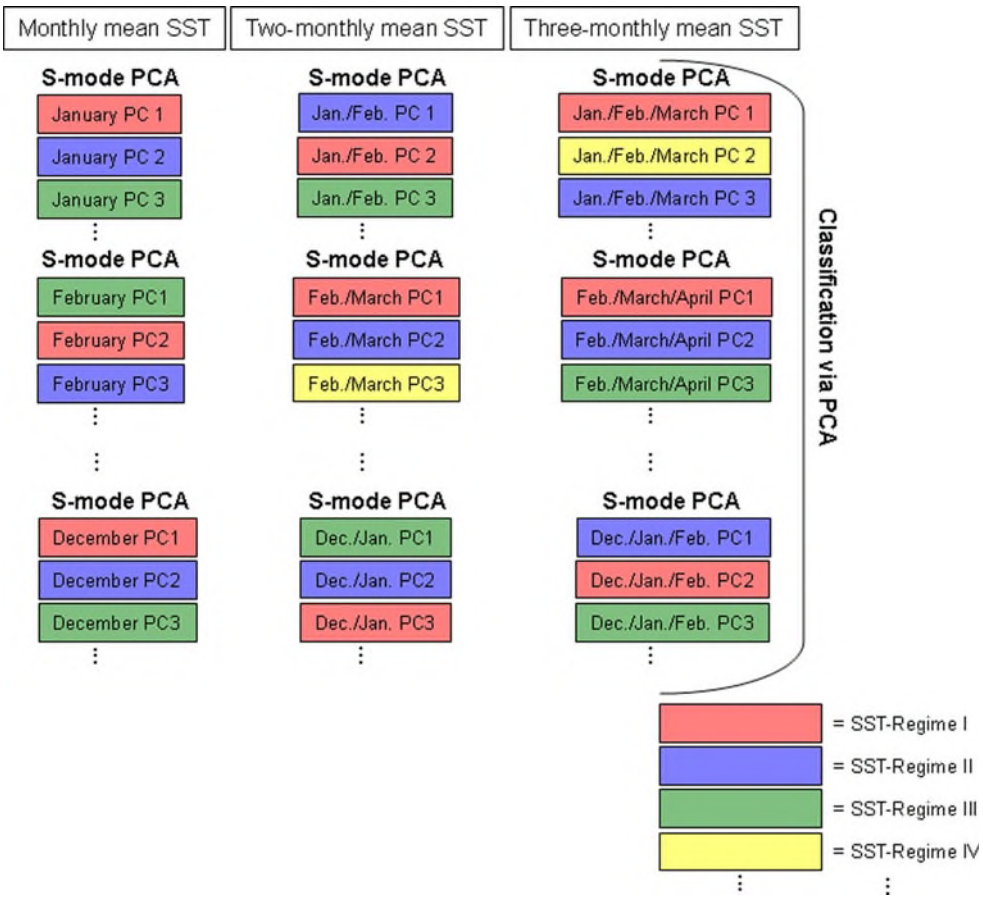

Fig. 1 Scheme of the methodology for the determination of the SST regimes. The assignments of PCs to specific SST-regimes are arbitrary and have been included only for illustration purposes. For detailed information see Sect. 3

the year or even for the whole year. The term 'regime' is used in this context for those large-scale patterns of SST variation persisting at least for a two-month season and showing a regular occurrence (a recurrent state). This can basically be transferred from the definitions of atmospheric modes, patterns, and regimes by Stephenson et al. (2004). One problem that may arise with this approach is the variability in strength and geographical location of the centres of SST variation for a particular regime from one sub-period to another. This can hamper the determination of distinct regimes and has to be accounted for by adequate techniques:

To classify the individual PC loading patterns into distinct regimes, a further PCA is performed. The input matrix consists of all PC loadings from the monthly mean, 2-monthly mean, and 3-monthly mean analyses, with the PCs as variables and the grid boxes as cases. This additional PCA groups the original PCs with similar loadings on the grid boxes, hence the PCs representing a similar SST variation. These new PCs generated within this PCA of the original loading patterns can be regarded as different SST regimes. The loading patterns from the PCAs of the original fields are assigned to the SST regimes by looking for the highest absolute loading of a variable among all new PCs and by searching for the highest absolute loading of a new PC on the different variables. If both values coincide, the original loading pattern of a sub-period correlates best with a particular regime (i.e. the original loading pattern is mostly similar to the regime loading pattern) and this loading pattern is the best fit for this sub-period.

Different runs of the PCA of the loading patterns are performed with different numbers of PCs to be extracted including all solutions between 2 and 39 PCs (the latter corresponds to approximately 95% of explained variance). This is done to rule out the possibility that the choice of a certain number of PCs affects the assignment of the loading patterns to the regimes. Results indicate that when extracting only a small number of PCs, loading patterns of different sub-periods are sometimes pooled in one regime, even though they cannot represent the seasonal cycle of the same regime due to the dissimilarity of the loading patterns. On the other hand, when extracting a large number of PCs it may happen that loading patterns of different months which definitely represent the same regime, are split into separate regimes. This splitting is due to a continued seasonal differentiation of a regime. In general, the uncertainties related to a correct assignment are the result of the intra-annual variability of a regime. This variability can be attributed to a

set of varying characteristics (like the dominance and intensity of a regime changing from month to month) as well as to internal variations such as the spatial position and strength of the particular centres of variation. Altogether, uncertain assignments of loading patterns to a regime concern about 5% of all loading patterns.

To decide whether a loading pattern belongs to a particular regime and whether certain seasonal regimes can be merged into one common regime, all possible solutions from 2 up to 39 PCs are taken into consideration. The final decision is made by generating prototypical loading patterns and by looking at the scores (time coefficients) of the corresponding PCs.

The prototypical loading pattern of a regime is defined as the mean loading pattern, averaged over all loading patterns belonging to this regime. Loading patterns which are candidates for a particular regime, but cannot be clearly assigned by using the above-described method, are correlated with the prototypical loading pattern. However, due to the large sample size (about 5,000 grid boxes) even relatively low amounts of correlation coefficients are statistically significant. Therefore, the significance of correlation coefficients cannot be used to decide on the similarity of two patterns. For that reason a method of Bland and Altman (1986), who compared medical test series, is adapted. At first the correlation coefficient of two loading patterns is calculated. As a minimum criterion of correspondence its absolute amount has to be >0.7 (common variance greater than approximately 50%). If this is the case, the mean difference of the loadings and the standard deviation of the differences between the two patterns are calculated. No substantial difference between the two loading patterns is assumed if less than 5% of all grid boxes are outside an area of agreement. The upper and lower boundaries of the area of agreement are determined by adding or subtracting twice the standard deviation from the mean difference. This method aims at the detection of strong differences between the correlated patterns regarding the spatial location and strength of the centres of variation (areas with high positive or negative loadings). If no differences can be identified, the loading pattern in question is assigned to the corresponding regime and a new prototypical loading pattern is calculated for this regime including this additional loading pattern. The finally resulting prototypes of all regimes indicate the mean characteristics of the prevailing tropical and northern hemisphere extratropical SST variation in the period 1950–2003. Altogether 21 SST-regimes can be identified by this approach, eleven for the Pacific Ocean, six for the Atlantic Ocean, two for the Indian Ocean, and two regimes with co-variations in different oceans. However, since there has been a major climatic shift observed in the Pacific region in the 1970s (Trenberth 1990, Miller et al. 1994, Wang 1995), the question arises whether these SST-regimes are stationary through time. This question is focussed in Sect. 4 leading to the exclusion of four non-stationary regimes. The remaining regimes are reproduced in Fig. 2 and described in Sect. 5.

Finally, the PC scores (time coefficients) are also taken into account, because we expect a certain temporal persistence for a regime. Therefore, the scores of those PCs of consecutive sub-periods being candidates for a particular regime are correlated to confirm the results obtained. A temporal persistence over several months is evident for most regimes, and the consideration of scores works well as an additional tool for the identification of SST regimes, in such a sense that the correlation of the scores confirms the results obtained by the techniques described above. But it is not unusual for the regimes that there are breaks during the seasonal progression. Such breaks are specified in more detail at the beginning of Sect. 5 based on examples reflecting the El-Niño variation and the North Atlantic Tripole.

4 Stationarity of SST-regimes

In order to address this issue, the whole study period from 1950 to 2003 is separated in two sub-intervals, leaving out the 1970s when the climate shift in the Pacific region has taken place. For each of the two 20-year sub-intervals (1950–1969, 1980–1999) the SST-regimes are re-determined, following the same methodology as described in Sect. 3.

Concerning four SST-regimes (three of the Pacific Ocean and one of the Atlantic Ocean), not all of the corresponding PCs can be identified in both sub-periods. The affected regimes are secondary regimes in such a sense that they only become apparent in a particular season and that the PCs being assigned to the regimes have explained variances of <3% in a particular month or monthly combination. Three of the non-stationary regimes have their centres of variation in the Pacific Ocean. More precisely one regime has its centre of variation in the North Pacific Ocean at around 30°N and 140°W–150°W. It is only evident during the summer months. The spatial focus of the other two Pacific regimes is in the tropical Pacific Ocean, one in the eastern Pacific Ocean, the other one in the western Pacific Ocean, being only existent from January to March. The fourth non-stationary regime has its centre of variation in the North Atlantic Ocean around the British Isles and occurs in the spring and autumn months. None of the four regimes shows higher cross correlation coefficients to indices of atmospheric modes. To account for the temporal non-stationarity of these four regimes, they are excluded from further analysis. Therefore, only 17

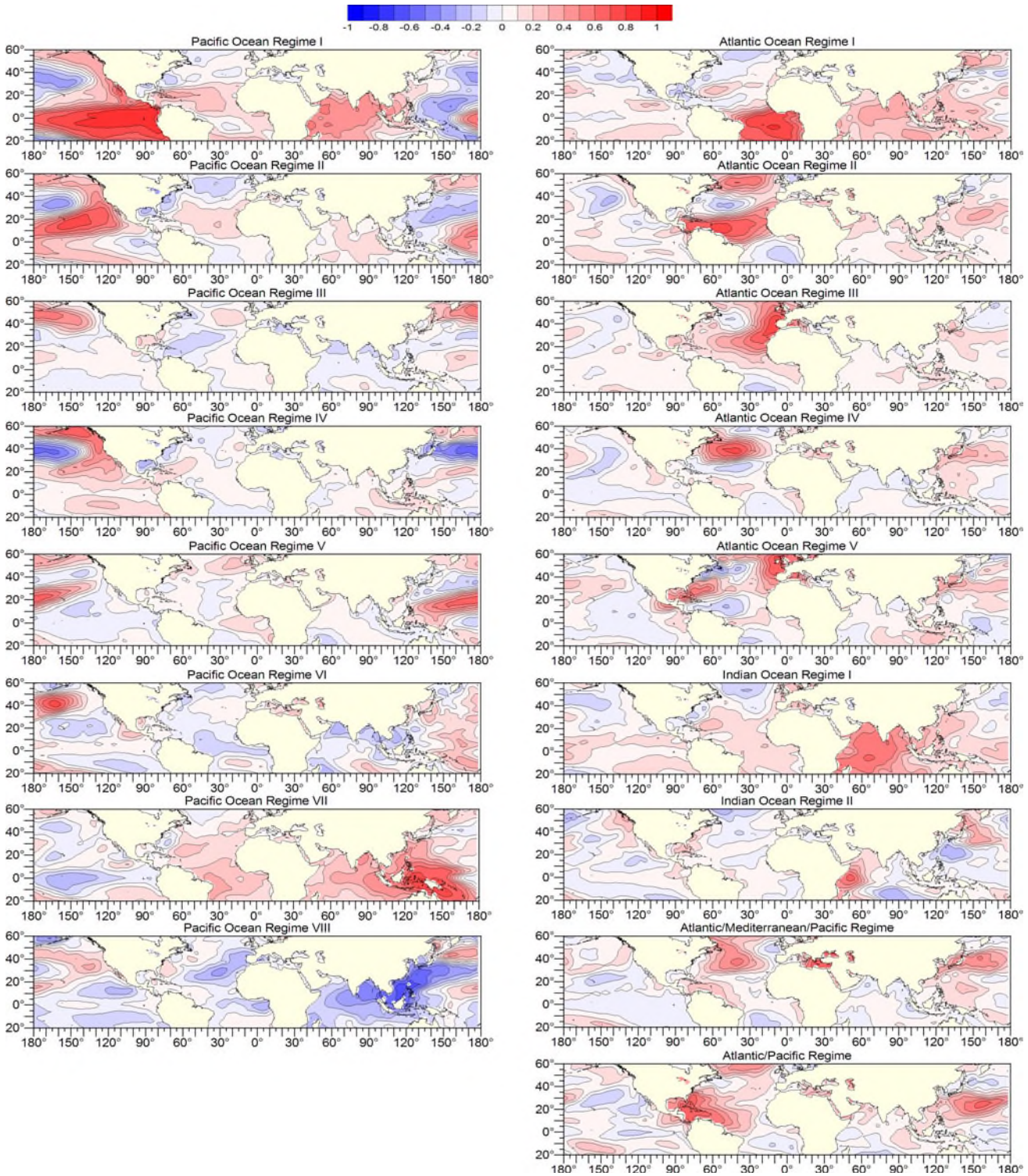

Fig. 2 Prototypical loading patterns of the SST-regimes, defined as the mean loading patterns averaged from the corresponding loading patterns of s-mode PCAs of monthly mean, 2-monthly mean and 3-monthly mean SST data in the period 1950–2003

SST-regimes are included in Fig. 2 and characterized in detail in the following section.

The analysis reveals that most of the SST-regimes are operating in both sub-periods. But some of the SST-regimes have different importance in these two intervals, indicated by differing amounts of explained variance of the PCs belonging to a certain regime. For the North Pacific Ocean for instance, the Pacific Ocean Regime II (see

Fig. 2) which describes parts of the tropical and subtropical SST-variability in the central North Pacific Ocean (see Sect. 5), gains importance in winter (December–February) during the later sub-period. This is indicated by an increase of explained variance of the corresponding PC from approximately 6% in 1950–1969 to 9.5% in 1980–1999 in relation to the total of explained variance of approximately 87% for the whole SST-variability in the study area from 20°S to 60°N. For the Atlantic Ocean, the corresponding Regime II gains importance during winter in the period 1980–1999 compared to 1950–1969, indicated by an increase of explained variance of the corresponding PCs of about 4% (from approximately 7% in the earlier sub-period to 11% in the later one). This may be explained by the strengthening of the positive mode of the North Atlantic Oscillation (NAO) in the later period, since the atmospheric NAO pattern is regarded to be strongly connected to the Atlantic Ocean Regime II.

Additionally, some regimes show varying PC-loadings outside the main centres of variation. This can be found for example for the Pacific Ocean Regime I which reflects the ENSO-phenomenon. In the years 1950–1969 higher positive loadings (besides the maximum in the eastern tropical Pacific Ocean) are present in the northern and central Indian Ocean dropping to distinctly lower values in the later sub-period from 1980 to 1999. In contrast to that, the centre of variation with opposite sign in the western tropical Pacific (centred around 10°N and 150°E–170°E) is more pronounced in the later sub-period. Regarding the loadings in extra-tropical latitudes, higher negative values are present in the North Atlantic Ocean during the period 1950–1969, but in the North Pacific Ocean during the period 1980–1999.

In conclusion, it should be pointed out that the variations of SST-regimes in the two sub-periods do not systematically affect the skill of monthly forecasts in temperature and precipitation of the Mediterranean area (being the ultimate aim of this study). The four examples which will be presented in detail in Sects. 5.1, 5.2, 6.1 and 6.2 of part II of this paper, do not show any significant differences regarding the mean skill of the forecasts in the two sub-periods 1950–1960 and 1980–1999. In fact, forecast performance does not indicate a major shift in the regime–climate-relationships in the 1970s, but rather seems to vary on intra- to inter-decadal timescales (see part II of this paper). This can be related to the forecast procedure selecting not only one SST-regime, but a combination of several regimes as predictors, so that specific variations in the SST–regime–climate-relationships can interfere with each other.

5 Characterization of SST-regimes

After excluding four non-stationary regimes (see Sect. 4), 17 SST-regimes remain to describe the prevailing SST variability. The centres of variation (areas of high absolute loadings) of eight regimes are located in the Pacific Ocean. These regimes can further be distinguished into one regime essentially describing the El-Niño-phenomenon, five regimes for the SST variation in the Northern Pacific, and two regimes with their centres of variation in the tropical and subtropical Western Pacific. For the Atlantic Ocean the SST variation is described by five regimes, one of them depicting a tropical anomaly in the southern hemisphere Atlantic Ocean, and four regimes characterizing the SST variation in the North Atlantic Ocean. Furthermore, two regimes are defined for the Indian Ocean, and two regimes show a distinct simultaneous SST variation in different ocean basins. Figure 2 shows the spatial patterns of these 17 SST-regimes, and Fig. 3 gives an overview of the regime occurrences (including percentages of explained variance) in all 1-, 2-, and 3-month periods of the year.

Some of the regimes exist, with varying strength and spatial extent, throughout the whole year, whereas other regimes are only characteristic for a particular season. Furthermore, the seasonal progression of regimes often shows distinct characteristics. For the example of the Pacific Ocean Regime I which reflects the ENSO-phenomenon, results of correlation analysis of consecutive sub-periods are presented in Fig. 4a. Obviously the loading patterns which belong to this SST regime, exhibit a high temporal persistence from early northern summer until the beginning of the next year, but from January to April there is a low correlation level of the time series, coinciding with the time of reorganisation of the tropical Pacific Ocean state in spring. However, the loading patterns of these months likewise display the ENSO-regime, indicated by high correlation coefficients with well-established Niño-Indices (Niño 1 + 2 Index, Extreme Eastern Tropical Pacific SST, 0°S–10°S, 90°W–80°W, and Niño 3 Index, Eastern Tropical Pacific SST, 5°N–5°S, 150°W–90°W).

As a further example, the correlation coefficients referring to the loading patterns of the Atlantic Ocean Regime II are displayed in Fig. 4b. The centres of SST variation of this tripole regime are located in the North Atlantic Ocean at approximately 10°N, 30°N, and 50°N (opposite sign of the loadings in the central part). This regime exhibits a high temporal persistence throughout most of the year with the exception from September to November. This low intra-annual persistence in the autumn months might be due to a seasonal modification of the factors governing the SST

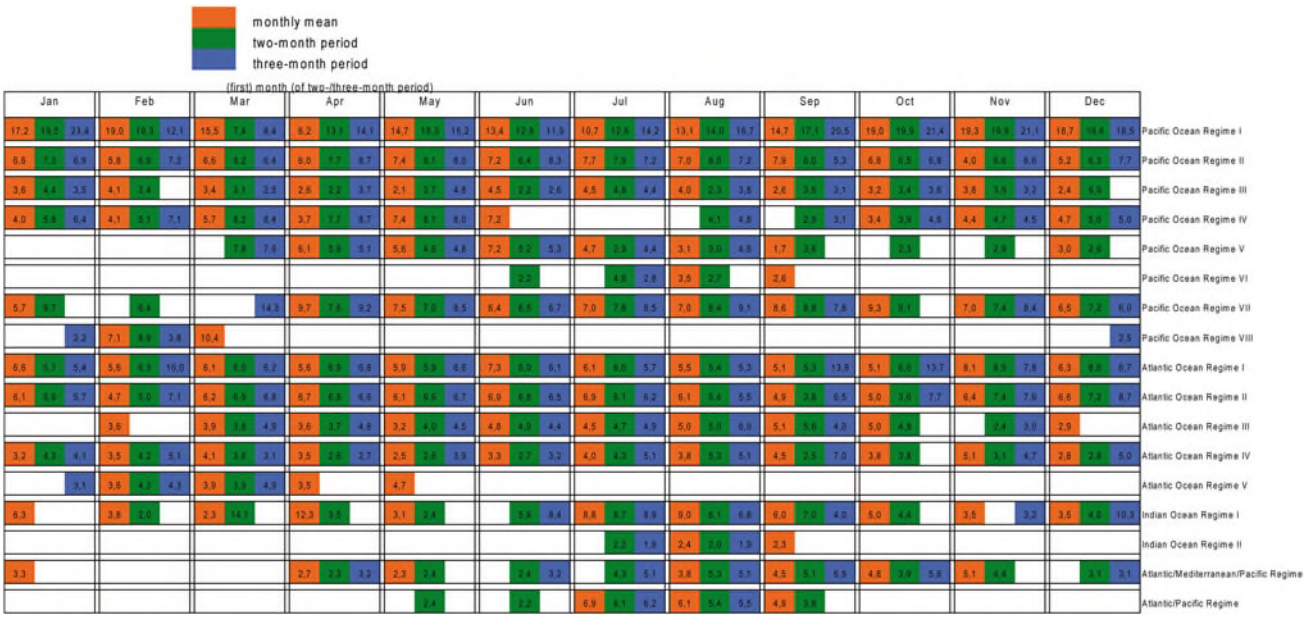

Fig. 3 Occurrence of the SST-regimes (*colour scale*) and percentages of explained variance of the corresponding PCs (*black numbers*) during 1-, 2-, and 3-month periods of the year

regime, e.g. caused by the disintegration of the seasonal thermocline (Cassou et al. 2004).

Further relevant characteristics of the SST-regimes will be summarized according to the different ocean basins.

5.1 Pacific Ocean regimes

The Pacific Ocean Regime I can be tracked over the whole year, i.e. its loading patterns are identified for all sub-periods of the year. It represents the ENSO-phenomenon as confirmed by correlation coefficients around 0.9 with the Niño 1 + 2 and Niño 3 Indices. The Pacific Ocean Regime I reproduces some of the well-known connections of ENSO to the atmospheric circulation of the North Pacific sector (e.g. Trenberth et al. 1998, Wang and Fu 2000, Liu and Alexander 2007), indicated by stronger cross correlation coefficients (>0.5/<−0.5) with various atmospheric indices for this region like the Pacific/North American Pattern (PNA), the East Pacific–North Pacific Pattern (EP–NP) and the West Pacific Pattern (WP) according to definitions from the NOAA Climate Prediction Center CPC (http://www.cpc.ncep.noaa.gov/data/teledoc/telecontents.shtml). Interestingly, higher correlations can also be established with the so-called Mediterranean Oscillation MO (Conte et al. 1989) during late summer and early autumn, in accordance with relationships between ENSO and the MO reported by Seubert and Jacobeit (2007). On the other hand, there is only a low correlation (not greater than 0.35) of the Pacific Ocean Regime I with the Tropical Northern Hemisphere pattern (TNH) which can be seen as an atmospheric fingerprint of ENSO in the northern extratropics. This might be due to the nonlinear relationship between ENSO and TNH, with a dominant connection of warm ENSO events to negative phases of the TNH. This nonlinear link may hamper a clear identification via linear correlation analysis used in the present study.

The Pacific Ocean Regime II which exists over the whole year is characterized by two centres of variation with opposite sign in the North Pacific Ocean. The time coefficients of this regime do not show higher correlations to the established SST-indices of this region like the Niño-Indices or the Pacific Decadal Oscillation (PDO, Mantua et al. 1997). The southern centre of variation which extends from the eastern North Pacific to the equatorial West Pacific, seems to trace the location of the North Equatorial Current and its upstream extensions. From April to June, and from November to December, its spatial location reveals some longitudinal variability with highest PC-loadings varying between 130°E and 160°E. This results in an elongated area of high PC-loadings in the mean loading pattern of Fig. 2. The northern centre of variation is located north of Hawaii between 30°N–40°N and 170°E–150°E. This second Pacific Ocean Regime might describe parts of the tropical and subtropical SST-variability in the central North Pacific Ocean which is not connected to the ENSO-variability represented by the first regime.

The centre of variation of the Pacific Ocean Regime III is located in the northern part at around 50°N and has a representative loading pattern in every sub-period of the year. Nakamura et al. (1997) point out that parts of the North Pacific SST variability are concentrated at the subarctic front. This region corresponds to the area with the

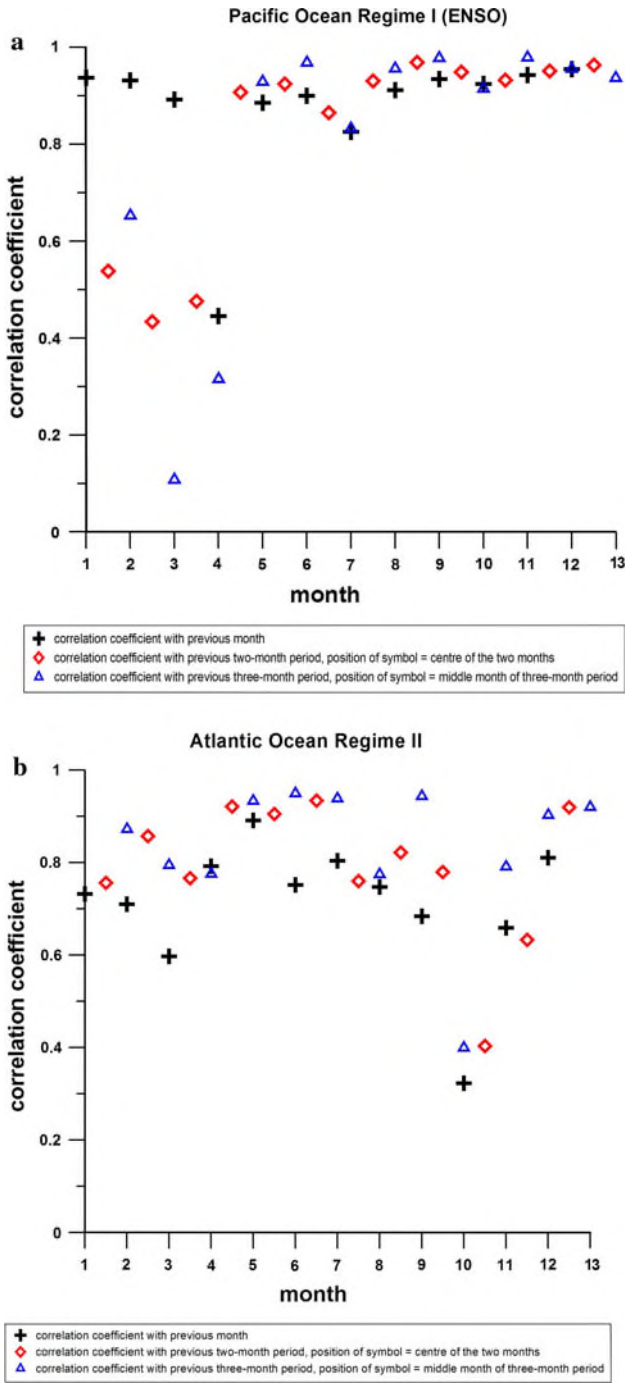

Fig. 4 Correlation coefficients of the SST regime time coefficients from consecutive 1-, 2-, and 3-month sub-periods. **a** Pacific Ocean Regime I. **b** Atlantic Ocean Regime II

highest SST-gradients in the North Pacific Ocean and is connected to the Subpolar Gyre. In the autumn months the Pacific Ocean Regime III develops higher correlations (>0.5) to atmospheric circulation patterns which are related to the Pacific polar Jetstream. Thus, it is generally located in an area of strong oceanic and atmospheric temperature gradients.

The Pacific Ocean Regime IV is linked to the Pacific Decadal Oscillation (PDO, Mantua et al. 1997) with correlation coefficients of about 0.8. In late summer and early autumn (July–September) the regime does not exist or becomes inconsistent. This intra-annual behaviour is also described by Alexander et al. (1999). The mean loading pattern of the regime also corresponds to the second Empirical Orthogonal Function from an EOF-analysis of the Pacific SSTs by Deser and Blackmon (1995). Various studies point to a correlation of the PDO with ENSO-variability (Alexander et al. 2002, Trenberth and Hurrell 1994) and with the (atmospheric) Pacific North American pattern (PNA; Wallace et al. 1992). In the present study higher cross correlation coefficients of about 0.6 become evident in winter with a lead time of about 1–2 months of the PNA pattern with regard to the Pacific Ocean Regime IV. However, correlation coefficients with the Niño-Indices are rather low (not exceeding 0.35).

The Pacific Ocean Regime V is characterized by a centre of variation aligned from southwest to northeast over the Pacific Ocean with its maximum at approximately 20°N. It can be identified mainly in the spring and summer months. The centre of variation is located between the North Equatorial Current and the Kuroshio-Current. Hence it can be seen to describe the temperature variation in the area of the oceanic subtropical front in these months. In summer the atmospheric patterns EP–NP and WP cross-correlate (coefficients of 0.5–0.6) with the time series of this SST-regime 1–2 months later, thus indicating an atmospheric influence on the regime development.

The centre of variation for the Pacific Ocean Regime VI is located around 40°N and 160°W. This regime is only present in the summer months. It appears to constitute the summertime counterpart of the PDO (corresponding to the Pacific Ocean Regime IV), when only the westerly centre of variation is developed in the surface layer (Alexander et al. 1999).

The Pacific Ocean Regime VII has an extended centre of variation in the tropical West Pacific existing throughout most of the year except of February and March when a second centre arises in the eastern Indian Ocean. This regime is somewhat related to the atmospheric circulation of the North Pacific sector, indicated by correlation coefficients of about 0.5 with the PNA and the East Pacific–North Pacific patterns in some months.

The centre of variation of the Pacific Ocean Regime VIII in the subtropical West Pacific with its focus in the South China Sea is only existent in the winter months. The time series of this ocean regime in March correlates with the atmospheric WP (West Pacific) pattern in the preceding months of January and February (correlation coefficient about 0.6). A connection of the SST-variation in this region

to the WP pattern in winter is also reported by Wallace et al. (1990).

5.2 Atlantic Ocean regimes

For the Atlantic Ocean, five SST regimes are included in Figs. 2 and 3. A first one, persisting during the whole year, has its centre of variation in the southern hemispheric tropical Atlantic Ocean at approximately 10°S (Atlantic Ocean Regime I). This centre of variation is also described by Houghton and Tourre (1992) as the leading mode of tropical Atlantic SST-variability. Several studies (Hirst and Hastenrath 1983, Zebiak 1993, Ruiz-Barradas et al. 2000, Keenlyside and Latif 2007) find that main characteristics in this region (increasing SSTs accompanied by an eastward shift of warm water, a relaxation of the equatorial trade winds in the central basin, and a southward shift of convection) resemble the El-Niño phenomenon of the Pacific Ocean, though weaker and with some distinguishing features. Therefore, this mode has been referred to as the Atlantic Niño. Its maximum SST anomalies occur in boreal summer, instead of boreal winter as in ENSO. Zebiak (1993) and others find no connection of the Atlantic Niño mode with ENSO. But Häkkinen and Mo (2002) suggest that SST-variability in this region is influenced by teleconnections with the Pacific area (mainly in spring and summer), and also Keenlyside and Latif (2007) obtain a significant correlation of Pacific and Atlantic SSTs in boreal spring mainly since the 1970s. Regarding ocean–atmosphere-couplings, Keenlyside and Latif (2007) point out that the atmosphere is primarily sensitive to eastern Atlantic SSTs only during spring and early summer. On the contrary, Häkkinen and Mo (2002) suggest that SST-variability in this region is influenced by the NAO mainly in winter. In the present study a correlation coefficient of about 0.6 can be established between the Atlantic Ocean Regime I in summer and the atmospheric East Atlantic Pattern with its major centre of variation above northern mid-latitudes in the preceding winter.

A second prominent pattern of Atlantic SST-variability (Atlantic Ocean Regime II) depicts two centres of variation in the North Atlantic Ocean between 10°N and 20°N and at approximately 50°N. In between a third centre with opposite sign is located in the western North Atlantic Ocean at about 30°N. This regime can be traced (with changing intensity) throughout the whole year, but with a low intra-annual persistence in autumn (see second paragraph at the beginning of Sect. 5). The two northern centres of variation correspond to a dipole pattern described by Deser and Blackmon (1993) based on an EOF-analysis of wintertime SSTs of the North Atlantic Ocean. The southern centre of variation can be seen in accordance with the second principal component of tropical Atlantic SST-variability identified by Houghton and Tourre (1992). Comprehensively, the Atlantic Ocean Regime II can be described as the North Atlantic Tripole Pattern incorporating parts of the tropical as well as of the northern hemispheric extratropical variability. The regime correlates with the Atlantic Tripole-Index of the Earth System Research Laboratory (Deser and Timlin 1997) with a coefficient of about 0.7 (averaged over all months). The Atlantic Tripole Pattern results as the first EOF of the SSTs in the area 10°N–70°N, 0°W–80°W and is seen in close relationship to the NAO (Peng et al. 2003). Czaja and Frankignoul (2002) find that the North Atlantic Tripole pattern in November–January is forced to a certain extent by the NAO with maximum covariance when the atmosphere leads the ocean by 1 month. This finding is also confirmed by García-Serrano et al. (2008). However, Peng et al. (2003) depict that in GCM-simulations the North Atlantic SST tripole can also induce a strong NAO-like response in the late cold season (February–April).

The Atlantic Ocean Regime III has a centre of variation in the eastern North Atlantic Ocean between 30°N and 50°N, next to the coast of North Africa and the Iberian Peninsula. This regime occurs in all seasons except winter. A similar pattern has been identified by Watanabe and Kimoto (2000) as the leading EOF-pattern in the North Atlantic Ocean during summer (June–August). Czaja and Frankignoul (2002) also identify a similar SST-pattern and describe it as the North Atlantic horseshoe (NAH) pattern. In Fig. 2 the centres of variation of the Atlantic Ocean Regime III are more centralized due to the calculation of an average prototypical pattern, but when looking at the individual loading patterns belonging to this regime, the resemblance to the NAH pattern becomes obvious. The NAH pattern in summer has an influence on the NAO in winter with an optimum lead time of the SST-pattern of 4 months (Czaja and Frankignoul 2002). Cassou et al. (2004) propose an intra-annual cycle with the NAH pattern as a bridge over summer for the year-to-year persistence of the NAO in winter. According to the present study the Atlantic Ocean Regime III in spring seems to be forced to a certain extent by the atmospheric circulation of the North Atlantic sector, indicated by cross correlation coefficients of about 0.7 with the NAO and the Mediterranean Oscillation (time lags of 1 month). In summer, the SST-regime can be related to the Scandinavian Pattern with negative geopotential height anomalies over Scandinavia and positive ones over Western Europe being linked with its positive mode.

The centre of variation for the Atlantic Ocean Regime IV is located in the central northern part at approximately 40°N. This regime exists throughout the whole year, but it reveals a low temporal persistence from April to June and from September to October. Cassou et al. (2004) document, that negative SST anomalies in this region in late summer are associated with the negative phase of the NAO in the

subsequent early winter. García-Serrano et al. (2008) derive a regression of the NAH pattern (corresponding to the Atlantic Ocean Regime III) onto the Atlantic SSTs from summer to winter. Thereby also cold SST anomalies over the central North Atlantic emerge in the same region where the centre of variation of the Atlantic Ocean Regime IV is located. In the present study a correlation with the Atlantic Multidecadal Oscillation (areal mean of 25°N–60°N and 7°W–75°W, Enfield et al. 2001) during winter with coefficients of about 0.65 is found. In addition, the SST regime shows cross correlations with time lags of 1 month in summer and about 5 months in winter with the atmospheric circulation of the North Atlantic region, mainly with respect to the East Atlantic Pattern.

The Atlantic Ocean Regime V includes various centres of variation in the North Atlantic Ocean. Positive anomalies in the positive mode are located in the Caribbean region as well as in the region around the British Isles and Europe. A centre of variation with opposite loadings is located offshore Newfoundland. This regime appears to reflect the SST-variations due to the existence of the Gulf Stream. The Caribbean centre is located in the area of origin of the Gulf Stream, the opposite anomaly at Newfoundland marks the northern boundary where the Labrador Current is integrated, and the centre in the eastern North Atlantic shows the extensions of the Gulf Stream. This regime is only existent in the late winter and spring months, during the time when the ocean mixed layer has produced large thermal anomalies in response to wintertime storms (Czaja and Marshall 2001); at the same time Gulfstream and Labrador Current exhibit a relatively low intensity and are shifted southwards in their preferred location (Hogg and Johns 1995).

5.3 Indian Ocean regimes

For the Indian Ocean, two SST regimes are included in Fig. 2. The Indian Ocean Regime I depicts its centre of variation in the western and central parts of the ocean. This regime has a very high spatial and temporal persistence from July to October, for the other months variations in the location of the centre are evident, representing a seasonal shifting of the loading maximum from south of the equator in winter to the northern Indian Ocean in summer. This spatial shifting may be seen in the context of the seasonal characteristics of the Indian monsoon system. In addition, cross correlation coefficients absolutely >0.5 can be observed with the Niño 3 Index (Eastern Tropical Pacific SST, 5°N–5°S, 150°W–90°W) and with the Niño 4 Index (Central Tropical Pacific SST, 5°N–5°S, 160°E–150°W). This indicates a relationship with lag times from three up to 6 months of the Indian Ocean SSTs to the large-scale dynamics of the tropical Pacific region which is also reported, e.g. by Yu and Lau (2005) based on a study with a coupled global circulation model. Correlations with other atmospheric indices point to some further teleconnections to the circulation over the North Pacific as well as the North Atlantic area. A response of the extratropical circulation in the North Atlantic sector to Indian Ocean SSTs is supported by atmospheric general circulation model experiments of Hoerling et al. (2004).

The Indian Ocean Regime II reveals a centre of variation in the western Indian Ocean which is only realised in summer. The spatial location of the centre can be seen in correspondence to the north-western pole of the Indian Ocean Dipole whose south-eastern pole is weaker and of opposite sign. The Indian Ocean Dipole represents the second Empirical Orthogonal Function (EOF) in the scope of an EOF-analysis of the Indian Ocean SSTs (Yamagata et al. 2003).

5.4 Co-variability ocean regimes

The Atlantic/Mediterranean/Pacific Regime is a first one with co-variations in different ocean basins. The centres of variation are located in the central North Atlantic Ocean, the eastern Mediterranean Sea and in the western North Pacific Ocean. The SST regime can be traced throughout the whole year with the exception of February and March. In the months from April to June mainly the centres of variation in the eastern Mediterranean and in the North Atlantic Ocean are distinctive. In late summer and autumn (from August to November) the regime is developed with all three centres. A distinct correlation (coefficient of about 0.6) of this regime in August with the East Atlantic (EA) pattern 1 month earlier indicates an atmospheric forcing of the SST regime. A visual comparison with the EA-pattern in July (http://www.cpc.noaa.gov/data/teledoc/ea_map.shtml) confirms a great similarity regarding the location and the sign of the centres of variation in the Atlantic and Pacific regions. Only the atmospheric centre over western North America and the adjacent Pacific Ocean is not reproduced in the SST-pattern.

A further regime which contains co-variations in different oceans is the Atlantic/Pacific Regime. The centres of variation are located in the subtropical western areas of both ocean basins. Thus, they are located in the area of origin of the Gulfstream and the Kuroshio Current, respectively. This regime only exists during summer from May to September. In these months the currents reach their maximum intensity in the areas of origin (Fuglister 1951).

6 Conclusions

SST-regimes—defined as large-scale patterns with a regular and at least seasonal occurrence—have been identified by

the multiple application of s-mode PCA to monthly, 2-monthly and 3-monthly mean SST-fields in the area 20°S–60°N. By this way not only the well-known dominant patterns of SST-variation became apparent, but also little-known regimes could be identified. The SST-regimes were studied in particular with respect to their temporal evolution throughout the whole year. After testing the stationarity of the SST-regimes by comparing two 20-year sub-periods, 17 regimes were maintained for the characterization of the SST-variations in the period 1950–2003. These regimes reflect stationary SST-variations, inter-annual modes modulated on decadal timescales or factors related to global warming are not considered.

For the Pacific Ocean eight SST-regimes have been identified. The first one strongly resembles the El Niño-phenomenon thus being the most prominent one. Five SST-regimes are related to the North Pacific Ocean. Some of them can be traced throughout the whole year (like the Pacific Ocean Regimes II and III), whereas the Regime IV (which is similar to the PDO) shows a break in the intra-annual progression. The Regimes V and VI even are characteristic only for specific seasons. Finally, two Pacific Ocean Regimes have been identified having their centres of variation in the tropical and subtropical western Pacific.

For the Atlantic Ocean five SST-regimes have been confirmed by the statistical analyses. One regime has its centre of variation in the tropical Atlantic Ocean, the other four regimes focus on the SST-variations in the North Atlantic. They include patterns which can be seen in connection to well-known modes of variation like the North Atlantic Tripole (reflected by Regime II) and the North Atlantic Horseshoe (corresponding to Regime III). The Atlantic Ocean Regime IV with its centre of variation in the central northern Atlantic at approximately 40°N can also be set in context to the intra-annual evolution of extratropical Atlantic SSTs. In contrast to that, Regime V describes a less-known pattern of variation, appearing in specific seasons of the year.

The SST-variations of the Indian Ocean are described by two regimes. The first one can be associated with the Indian monsoon system as well as with ENSO. The second regime includes some features of the Indian Ocean Dipole.

Finally, two SST-regimes have been identified which show co-variations in different ocean basins. One regime has its centre of variation in the Atlantic Ocean, the Mediterranean Sea, and the Pacific Ocean. It appears to depend on the atmospheric circulation of the North Atlantic/North Pacific sector. The other regime exhibiting co-variations in the North Atlantic and the North Pacific Oceans might be related to the western boundary currents, the Gulf Stream and the Kuroshio, respectively.

Despite the fact that the detection of specific modes of SST-variation has experienced considerable progress, there is still a major lack of knowledge how these patterns are forced in detail. Many results point to an atmospheric forcing of the SST-patterns (e.g. for the Pacific Ocean by Trenberth and Hurrell 1994, Wallace et al. 1992, Emery and Hamilton 1985, for the Atlantic Ocean by Czaja and Marshall 2001, Palmer and Zhaobo 1985, for the Indian Ocean by Luis and Kawamura 2001). This is also indicated in the present study by cross-correlations of SST-regimes to specific atmospheric circulation patterns with the atmosphere mostly leading the ocean. Nevertheless, particular SST-patterns can also be identified influencing the atmosphere, see for example Yulaeva et al. (2001) for the Pacific Ocean, Czaja and Frankignoul (2002) and Peng et al. (2003) for the Atlantic Ocean, Yuan et al. (2008) and Hoerling et al. (2004) for the Indian Ocean. The latter relationships are of special interest regarding seasonal predictions of regional climate. Therefore, the time coefficients of the SST-regimes have also been analysed with respect to their suitability as predictors for monthly precipitation and temperature in the Mediterranean area. This is described in part II of this paper.

Acknowledgments Financial support was provided by the DFG (German Research Foundation) under contract JA 831/3-1.

References

Alexander MA, Deser C, Timlin MS (1999) The reemergence of SST anomalies in the North Pacific Ocean. J Clim 12:2419–2433

Alexander MA, Bladé I, Newman M, Lanzante JR, Lau N-C, Scott JD (2002) The atmospheric bridge: the influence of ENSO teleconnections on air–sea interaction over the global oceans. J Clim 15:2205–2231

An S-I (2009) A review of interdecadal changes in the nonlinearity of the El Niño-Southern Oscillation. Theor Appl Climatol 97:29–40

Barnston AG, Smith TM (1996) Specification and prediction of global surface temperature and precipitation from global SST using CCA. J Clim 9:2660–2697

Bland JM, Altman DG (1986) Statistical methods for assessing agreement between two methods of clinical measurement. Lancet 8476:307–310

Cassou C, Deser C, Terray L, Hurrell JW, Drévi M (2004) Summer sea surface temperature conditions in the North Atlantic and their impact upon the atmospheric circulation in early winter. J Clim 17:3349–3363

Colman A, Davey M (1999) Prediction of summer temperature, rainfall and pressure in Europe from preceding winter North Atlantic Ocean temperature. Int J Climatol 19:513–536

Conte M, Giuffrida S, Tedesco S (1989) The Mediterranean oscillation: impact on precipitation and hydrology in Italy. In: Proceedings of the conference on climate and water. Publications of the Academy of Finland, Helsinki, pp 121–137

Czaja A, Frankignoul C (2002) Observed impact of Atlantic SST anomalies on the North Atlantic oscillation. J Clim 15:606–623

Czaja A, Marshall J (2001) Observations of atmosphere–ocean coupling in the North Atlantic. Quart J Roy Meteorol Soc 127:1893–1916

Deser C, Blackmon ML (1993) Surface climate variations over the North Atlantic Ocean during winter: 1900–1989. J Clim 6:1743–1753

Deser C, Blackmon ML (1995) On the relationship between tropical and north Pacific sea surface temperature variations. J Clim 8:1677–1680

Deser C, Timlin MS (1997) Atmosphere–ocean interaction on weekly timescales in the North Atlantic and Pacific. J Clim 10:393–408

Dix MR, Hunt BG (1995) Chaotic influences and the problem of deterministic seasonal prediction. Int J Climatol 15:729–752

Emery WJ, Hamilton K (1985) Atmospheric forcing of interannual variability in the Northeast Pacific Ocean: connections with El Niño. J Geophys Res 90(C1):857–868

Enfield DB, Mestas-Nunez AM, Trimble PJ (2001) The Atlantic multidecadal oscillation and its relationship to rainfall and river flows in the continental U.S. Geophys Res Lett 28:2077–2080

Fuglister FC (1951) Annual variations in current speeds in the Gulf Stream system. J Mar Res 10:119–127

García-Serrano J, Losada T, Rodríguez-Fonseca B, Polo I (2008) Tropical Atlantic variability modes (1979–2002). Part II. Time-evolving atmospheric circulation related to SST-forced tropical convection. J Clim 24:6476–6497

Häkkinen S, Mo KC (2002) The low-frequency variability of the Tropical Atlantic Ocean. J Clim 15:237–250

Hirst AC, Hastenrath S (1983) Atmosphere–ocean mechanisms of climate anomalies in the Angola–tropical Atlantic sector. J Phys Oceanogr 13:1146–1157

Hoerling MP, Hurrell JW, Xu T, Bates GT, Phillips AS (2004) Twentieth century North Atlantic climate change. Part II. Understanding the effect of Indian Ocean warming. Clim Dyn 23:391–405

Hogg NG, Johns WE (1995) Western boundary currents. U.S. National Report to International Union of Geodesy and Geophysics 1991–1994. Rev Geophys 33(Suppl):1311–1334

Houghton RW, Tourre YM (1992) Characteristics of low-frequency sea surface temperature fluctuations in the Tropical Atlantic. J Clim 5:765–772

Hwang S-O, Schemm J-K, Barnston A, Kwon W-T (2001) Long-lead seasonal forecast skill in far eastern Asia using canonical correlation analysis. J Clim 14:3005–3016

Keenlyside NS, Latif M (2007) Understanding equatorial Atlantic interannual variability. J Clim 20:131–142

Liu Z, Alexander M (2007) Atmospheric bridge, oceanic tunnel, and global climatic teleconnections. Rev Geophys 45:RG2005. doi:10.1029/2005RG000172

Lloyd-Hughes B, Saunders M (2002) Seasonal prediction of European spring precipitation from El Nino–Southern Oscillation and local sea-surface temperatures. Int J Climatol 22:1–14

Luis A, Kawamura H (2001) Characteristics of atmospheric forcing and SST cooling events in the Gulf of Mannar during winter monsoon. Remote Sens Environ 77:139–148

Mantua NJ, Hare SR, Zhang Y, Wallace JM, Francis RC (1997) A Pacific interdecadal climate oscillation with impacts on salmon production. Bull Am Meteorol Soc 78:1069–1079

Mason S, Mimmack G (2002) Comparison of some statistical methods of probabilistic forecasting of ENSO. J Clim 15:8–29

Miller AJ, Cayan DR, Barnett TP, Graham NE, Oberhuber JM (1994) The 1976–1977 climate shift of the Pacific Ocean. Oceanography 7:21–26

Moron V, Plaut G (2003) The impact of El Niño-southern oscillation upon weather regimes over Europe and the North Atlantic during boreal winter. Int J Climatol 23:363–379

Nakamura H, Lin G, Yamagata T (1997) Decadal climate variability in the North Pacific during the recent decades. Bull Am Meteorol Soc 78:2215–2225

Neelin JD, Battisti D, Hirst AC, Jin FF, Wakata Y, Yamagata T, Zebiak SE (1998) ENSO theory. J Geophys Res C104:14262–14290

Palmer TN, Zhaobo Sun (1985) A modelling and observational study of the relationship between sea surface temperature in the North-West atlantic and the atmospheric general circulation. Quart J Roy Meteorol Soc 111:947–975

Peng S, Robinson WA, Li S (2003) Mechanisms for the NAO responses to the North Atlantic SST Tripole. J Clim 16:1987–2004

Philipp A, Della-Marta PM, Jacobeit J, Fereday DR, Jones PD, Moberg A, Wanner H (2007) Long term variability of daily north atlantic-european pressure patterns since 1850 classified by simulated annealing clustering. J Clim 20(16):4065–4095

Rayner NA, Parker DE, Horton EB, Folland CK, Alexander LV, Rowell DP, Kent EC, Kaplan A (2003) Global analyses of sea surface temperature, sea ice, and night marine air temperature since the late nineteenth century. J Geophys Res 108:4407

Reynolds RW, Rayner NA, Smith TM, Stokes DC, Wang W (2002) An improved in situ and satellite SST analysis for climate. J Clim 15:1609–1625

Rodriguez-Fonseca B, Polo I, Serrano E, Castro M (2006) Evaluation of the North Atlantic SST forcing on the European and Northern African winter climate. Int J Climatol 26:179–191

Rodwell MJ, Rowell DP, Folland CK (1999) Oceanic forcing of the wintertime North Atlantic Oscillation and European climate. Nature 398:320–323

Rowell DP (1998) Assessing potential seasonal predictability with an ensemble of multidecadal GCM simulations. J Clim 11:109–120

Ruiz-Barradas A, Carton JA, Nigam S (2000) Structure of interannual-to-decadal climate variability in the Tropical Atlantic sector. J Clim 13:3285–3297

Seubert S, Jacobeit J (2007) Tropical influences on Mediterranean precipitation variability. Geophys Res Abstr 9

Smith TM, Reynolds RW (2003) Extended reconstruction of global sea surface temperatures based on COADS data (1854–1997). J Clim 16:1495–1510

Stephenson DB, Hannachi A, O'Neil A (2004) On the existence of multiple climate regimes. Quart J Roy Meteorol Soc 130:583–605

Trenberth KE (1990) Recent observed interdecadal climate changes in the Northern Hemisphere. Bull Am Meteorol Soc 71:993–998

Trenberth KE, Hurrell JW (1994) Decadal atmosphere–ocean variations in the Pacific. Clim Dyn 9:303–319

Trenberth KE, Branstator GW, Karoly D, Kumar A, Lau N-C, Ropelewski C (1998) Progress during TOGA in understanding and modeling global teleconnections associated with tropical sea surface temperatures. J Geophys Res 103(14):291–324

Wallace JM, Smith C, Jiang Q (1990) Spatial patterns of atmosphere–ocean interaction in the Northern Winter. J Clim 3:990–998

Wallace JM, Smith C, Bretherton CS (1992) Singular value decomposition of wintertime sea surface temperature and 500-mb height anomalies. J Clim 5:561–576

Wang B (1995) Interdecadel changes in El Nino onset in the last four decades. J Clim 8:267–285

Wang H, Fu R (2000) Winter monthly mean atmospheric anomalies over the North Pacific and North America associated with El Nino SSTs. J Clim 13:3435–3447

Watanabe M, Kimoto M (2000) On the persistence of decadal SST Anomalies in the North Atlantic. J Clim 13:3017–3028

Webster PJ, Moore AM, Loschnigg JP, Leben RR (1999) Coupled ocean-atmosphere dynamics in the Indian Ocean during 1997–1998. Nature 401:356–360

Woodruff SD, Diaz HF, Elms JD, Worley SJ (1998) COADS release 2 data and metadata enhancements for improvements of marine surface flux fields. Phys Chem Earth 23:517–527

Yuan Y, Yang H, Zhou W, Li C (2008) Influences of the Indian Ocean dipole on the Asian summer monsoon in the following year. Int J Climatol. doi:10.1002/joc.1678

Yamagata T, Behera SK, Rao SA, Guan Z, Ashok K, Saji HN (2003) Comments on "dipoles, temperature gradient, and tropical climate anomalies". Bull Am Meteorol Soc 84:1418–1422

Yu J-Y, Lau KM (2005) Contrasting Indian Ocean SST variability with and without ENSO influence: a coupled atmosphere–ocean GCM study. Meteorol Atmos Phys 90:179–191

Yulaeva E, Schneider N, Pierce DW, Barnett TP (2001) Modeling of North Pacific climate variability forced by oceanic heat flux anomalies. J Clim 14:4027–4046

Zebiak SE (1993) Air–sea interaction in the equatorial Atlantic region. J Clim 6:1567–1586

Zhang Y, Norris JR, Wallace JM (1998) Seasonality of large-scale atmosphere–ocean interaction over the North Pacific. J Clim 11:2473–2481